Coexisting Forms of Coupling and Phase-Transitions in Physiological Networks

2 authors, including:

Plamen Ch. Ivanov
Boston University
202 PUBLICATIONS   **23,474** CITATIONS

Some of the authors of this publication are also working on these related projects:

Cardiorespiratory coupling during sleep View project

Network Physiology and Nework Medicine, focus issue in the New Journal Physics View project

Coexisting Forms of Coupling
and Phase-Transitions in Physiological Networks

Ronny P. Bartsch[1,2,3] and Plamen Ch. Ivanov[1,3,4,*]

[1] Harvard Medical School and Division of Sleep Medicine, Brigham and Women's
Hospital, Boston, MA 02115, USA
[2] Department of Physics, Bar-Ilan University, Ramat Gan, 52900, Israel
[3] Department of Physics, Boston University, Boston, MA 02215, USA
[4] Institute of Solid State Physics, Bulgarian Academy of Sciences,
Sofia 1784, Bulgaria
plamen@buphy.bu.edu

Abstract. Utilizing methods from nonlinear dynamics and a network approach we investigate the interactions between physiologic organ systems. We demonstrate that these systems can exhibit multiple forms of coupling that are independent from each other and act on different time scales. We also find that physiologic systems interaction is of transient nature with intermittent "on" and "off" periods, and that different forms of coupling can simultaneously coexist representing different aspects of physiologic regulation. We investigate the network of physiologic interactions between the brain, cardiac and respiratory systems across different sleep stages, well-defined physiologic states with distinct neuroautonomic regulation, and we uncover a strong relationship between network connectivity, patterns in network links strength and physiologic function. We show that physiologic networks exhibit pronounced phase transitions associated with reorganization in network structure and links strength in response to transitions across physiologic states.

Keywords: Cardio-respiratory coupling, phase synchronization, sleep, networks.

1   Introduction

Physiologic organ systems exhibit complex nonlinear dynamics characterized by nonstationary, intermittent, scale-invariant and multifractal behaviors [1–6]. These dynamics result from underlying feedback mechanisms of neural regulation acting over a range of time scales [7–9] and exhibit pronounced phase transitions associated with changes across physiologic states and pathologic conditions [10–12]. Further, nonlinear coupling and interactions between organ systems influence their output dynamics and coordinate their functions, leading to another level of complexity. It is an open problem to adequately determine interactions

---

* Correspondence author.

between complex systems where their coupling is not known a priori, and where the only available information is contained in the output signals of the systems. For integrated physiological systems, this is further complicated by transient non-linear characteristics and continuous fluctuations in their dynamics. In recent years, research in nonlinear dynamics has focused on developing an analytic framework and novel measures to detect and quantify interactions between physiologic systems and to elucidate the nature of their coupling [13–15].

Here we hypothesize that integrated organ systems can communicate through several independent mechanisms of interaction which operate at different time scales, and that different forms of coupling can simultaneously coexist. Because the neuroautonomic regulation of each organ system changes with transition from one physiologic state to another leading to transitions in scaling and non-linear features of the output dynamics [12, 16–19], we further hypothesize that physiologic coupling also undergoes phase transitions in order to facilitate and optimize organ interactions during different physiologic states. Specifically, we hypothesize that at any given moment pairs of systems interact through complementary forms of coupling that may exhibit different strength and different stratification patterns across physiologic states.

2 Data and Methods

Data: To test our hypotheses, we analyze physiologic data recordings from a group of 189 healthy subjects (99 female and 90 male, ages ranging from 20-95 years) during night-time sleep (average record duration is 7.8 h), tracking changes in physiologic coupling across different sleep stages. We focus on physiological dynamics during sleep as sleep stages are well-defined physiological states, and external influences due to physical activity or sensory inputs are reduced during sleep. Sleep stages are scored in 30 s epochs by sleep lab technicians based on standard Rechtschaffen & Kales criteria. We consider EEG, ECG and respiratory signals. In particular, we focus on cardio-respiratory coupling and on the network of interactions between different brain areas and the cardiac and respiratory system.

Methods: Cardiac, respiratory and brain dynamics exhibit transient changes associated with different physiologic states and conditions. How their coupling responds to these changes in relation to the underlying mechanisms of physiologic control remains not understood. Moreover, whether the systems interact via different functional forms of coupling and whether these forms of coupling are influenced differently by the same physiologic state, is not known.

Employing ideas from the theory of non-equilibrium systems [22], synchronization of coupled nonlinear systems [14], time delay stability [23] and complex networks [24], we investigate aspects of physiologic coupling and networks of interaction between physiological systems, and how they change with transitions from one physiologic state to another.

Specifically, we investigate three forms of cardio-respiratory interaction and how they change during different sleep stages. Utilizing multichannel physiologic
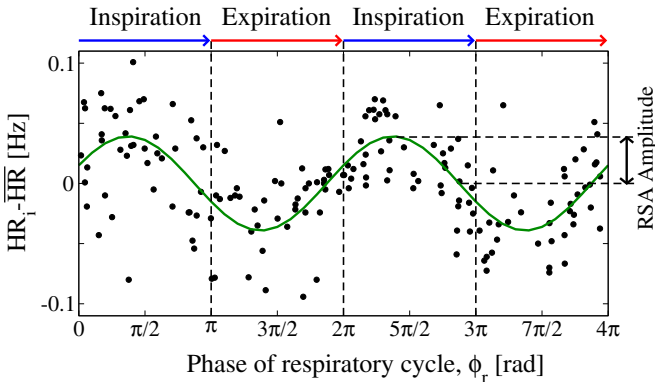
Fig. 1. Cardio-respiratory coupling: Respiratory sinus arrhythmia (RSA)
This form of coupling is characterized by a periodic variation of the heart rate (HR)
within each breathing cycle: increase of HR with inspiration and decrease of HR with
expiration for normal breathing frequencies ($\approx$ 7-12 breaths per min). The strength of
the coupling is defined by the amplitude of the HR variation measured relative to the
mean heart rate $\overline{\mathrm{HR}}$, called RSA amplitude. RSA is most pronounced at low breathing
frequencies and nonlinearly decreases with increasing breathing frequency [20, 21]. Data
points represent instantaneous heart rate (inverse heartbeat intervals), normalized to
the mean heart rate $\overline{\mathrm{HR}}$ within each breathing cycle, for a period of 200 sec over pairs
of consecutive breathing cycles. RSA is highlighted by a sinusoidal least-square-fit line
to the data points. Data are recorded from a healthy subject during sleep.

data during sleep as an example, we demonstrate that a network approach to
physiological interactions is necessary to understand how modulations in the reg-
ulatory mechanism of individual systems translate into reorganization of physi-
ological interactions across the human organism.

Respiratory sinus arrhythmia (RSA): In physiological studies, the interaction
between the cardiac and the respiratory system, is traditionally identified through
the respiratory sinus arrhythmia (RSA), which accounts for the periodic vari-
ation of the heart rate within a breathing cycle [20, 25]. Typically, for normal
breathing rates in the range 7-12 breaths per minute, RSA is characterized by
the increase of heart rate during inspiration and decrease during expiration, and
is quantified by the amplitude of this heart rate modulation. To obtain the RSA
amplitude, we first estimate the instantaneous heart rate (inverse heartbeat RR
interval) associated with each heartbeat within a breathing cycle, and from each
instantaneous heart rate we subtract the average heart rate for this breathing
cycle. We consider artifact-free segments of consecutive normal heartbeats with
duration $\geq$300 sec. We plot the instantaneous heart rates (normalized to the
mean) for each pair of consecutive breathing cycles within each artifact-free
data segment (Fig. 1), and we define the RSA amplitude as one half of the peak-
through difference in the least-square-fit sinusoid line to the data points. This
fit line represents the respiratory modulation of the heart rate (Fig. 1).

For our RSA analysis, heartbeat data (R-peaks) were extracted from the ECGs utilizing a semi-automatic peak detector (*Raschlab*, www.librasch.org). RR time intervals were calculated between each pair of consecutive R-peaks. A RR interval was labeled as artifact and excluded from the analysis if (i) the interval was shorter than 300 ms or longer than 2000 ms, or (ii) the interval was more than 30% shorter or more than 60% longer than the preceding RR interval. These exclusion criteria effectively eliminate ectopic heartbeats and artifacts. Respiration was measured by the oronasal airflow through a thermistor and by belts around the chest and abdomen. These three respiratory signals were resampled to 4Hz to eliminate high frequency fluctuations and to assure that the signal is narrow-banded, and thus its Hilbert transform can be used to calculate the respiratory phase.

Cardio-respiratory phase synchronization (CRPS): Phase-synchronization analysis was recently developed to identify interrelations between the output signals of coupled nonlinear oscillatory systems even when these output signals are not cross-correlated [14, 26, 27]. Thus, phase-synchronization analysis can quantify the degree of coupling between nonlinear systems when other conventional methods can not.

Cardio-respiratory synchronization can systematically be studied in an automated way by utilizing an algorithm that evaluates cardio-respiratory synchrograms (Fig. 2(d)). The synchrogram is a method in which the phase of a continuous signal (e.g., respiration $r(t)$) is plotted at incidents t_k of a second signal described by a point process (e.g., the occurrence of R-peaks in the ECG at times t_k). The instantaneous respiratory phase $\phi_r(t)$ can be calculated by the analytic signal approach [26] and, in the complex plane, $\phi_r(t)$ represents the angle between the respiratory signal $r(t)$ and its Hilbert transform $r_H(t)$ which is the imaginary part of the respiratory signal (Fig. 2(c)). The plot of $\phi_r(t_k)$ over t_k defines the cardio-respiratory synchrogram (Fig. 2(d)). Cardio-respiratory phase synchronization exists when n parallel horizontal lines are observed, where n is the number of heartbeats per breathing cycle ($n = 3$ in Fig. 2(d)). In our automated synchrogram algorithm, the times t_k of the occurrence of heartbeats are mapped on the cumulative respiratory phase $\Phi_r(t)$, and $\phi_r^m(t_k) = \Phi_r(t)$ mod $2\pi m$ is plotted versus t_k. For each m respiratory cycles where n heartbeats occur at times t_i^c (t_i^c corresponds to the times of $i = 1, \ldots, n$ heartbeats within m respiratory cycles, denoted by c), we replace the phase points $\phi_r^m(t_i^c)$ by averages $\langle \phi_r^m(t_i^c) \rangle$ and standard deviations $\sigma(t_i^c)$ calculated over all phase points in the time window $\mathfrak{T}_i^c = [t_i^c - \tau/2, t_i^c + \tau/2]$ and in the phase interval $\mathfrak{R}_i = [\phi_r^m(t_i^c) - \frac{2\pi m}{n}, \phi_r^m(t_i^c) + \frac{2\pi m}{n})$ (i.e., we average the phase points along the horizontal lines in Fig. 2(d) over the time window $\mathfrak{T}_i^c$). Thus, the phase average and standard deviation are defined by $\langle \phi_r^m(t_i^c) \rangle = \frac{1}{N_i} \sum_{t_k \in \mathfrak{T}_i^c} \phi_r^m(t_k)$ and

$\sigma(t_i^c) = \sqrt{\frac{1}{N_i} \sum_{t_k \in \mathfrak{T}_i^c} (\phi_r^m(t_k) - \langle \phi_r^m(t_i^c) \rangle)^2}$, where N_i is the number of phase points (heartbeats) in the time window $\mathfrak{T}_i^c$ and the phase interval $\mathfrak{R}_i$, and where m is the number of respiratory cycles in which n heartbeats occur. Next, for each breathing cycle we average the standard deviation $\sigma(t_i^c)$ for all $i = 1, \ldots, n$
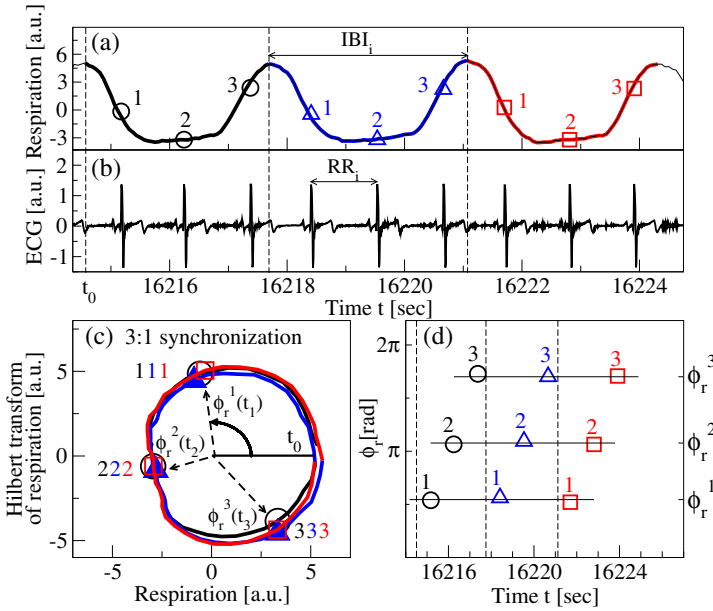
Fig. 2. Cardio-respiratory coupling: Phase synchronization (CRPS) Three consecutive breathing cycles (in black, blue and red) are shown in (a) and a simultaneously recorded ECG signal in (b). The interbreath interval (IBI) is approximately 3 times longer than the beat-to-beat interval (RR). Horizontal arrows indicate an interbreath interval (IBI) and a RR beat-to-beat interval. (c) Demonstration of $3:1$ phase synchronization between the heartbeats and respiratory cycles shown in (a) and (b). For each breathing cycle the 1st heartbeat occurs at the same respiratory phase $\phi_r^1(t)$, and the 2nd and 3rd heartbeats within each cycle occur at $\phi_r^2(t)$ and $\phi_r^3(t)$ (symbols collapse), indicating robust CRPS. (d) Three horizontal parallel lines formed respectively by the 1st, 2nd and 3rd heartbeats in the three consecutive breathing cycles indicate $3:1$ phase synchronization. Different symbols represent heartbeats in different breathing cycles as in (a) and (c), and vertical dashed lines show the beginning of each breathing cycle.

phase points $\langle\phi_r^m(t_i^c)\rangle$ to obtain $\langle\sigma\rangle_n$. Only breathing cycles with $\langle\sigma\rangle_n \leq \frac{2\pi m}{n\Delta}$ are considered, and synchronization segments are identified only when such consecutive breathing cycles span over time intervals $\geq T$. Finally, we relate the phase synchronization segments to the time intervals of the different sleep stages throughout the night, and for each sleep stage we calculate the % synchronization as the ratio between the time duration of the sum of all synchronization segments and the total time duration of the sleep stage during the night. Segments of data artifacts in both cardiac and respiratory signals are disregarded in these calculations. Since we have three respiratory signals from oronasal airflow, chest and abdomen belts, for each consecutive episode in a given sleep stage we consider the pair of cardiac and respiratory signals that yields the highest % synchronization (thus, optimally reducing the influence of breathing artifacts).

In our analyses we use $\Delta = 5$, and $T = \tau = 30$ sec corresponding to standard 30 sec sleep-stage scoring epochs.

For the phase-synchronization analysis we used the same signal pre-processing procedure for the heart rate and respiratory signals as described for the RSA analysis.

Time delay stability analysis (TDS): Integrated physiologic systems are coupled by feedback and/or feed forward loops with a broad range of time delays. To probe physiologic coupling we propose an approach based on the concept of time delay stability [23]: in the presence of strong stable interactions between two systems, transient modulations (e.g., bursts) in the output signal of one system lead to corresponding changes that occur with a stable time lag in the output signal of another coupled system. Long periods of constant time delay indicate strong physiologic coupling. We demonstrate the TDS method on the example of cardio-respiratory interaction, considering the time delay interrelation between bursts in the heart rate and the respiratory rate (Fig. 3(a,b)).

The TDS method consists of the following steps:
(1.) To probe the interaction between two physiological systems X and Y, we consider their output signals $\{x\}$ and $\{y\}$ each of length N and sampled at 1 Hz. We divide both signals $\{x\}$ and $\{y\}$ into N_L overlapping time windows ν of equal length $L = 60$ sec. We choose an overlap of $L/2 = 30$ sec which corresponds to the time resolution of the conventional sleep-stage scoring epochs, and thus $N_L = [2N/L] - 1$. Prior to the analysis, the signal in each time window ν is normalized separately to zero mean and unit standard deviation, in order to remove constant trends in the data and to obtain dimensionless signals. This normalization procedure assures that the estimated coupling between the signals $\{x\}$ and $\{y\}$ is not affected by the difference in their amplitudes.
(2.) Next, within each time window $\nu = 1, \ldots, N_L$, we calculate the cross-correlation function $C_{xy}^{\nu}(\tau) = \frac{1}{L} \sum_{i=1}^{L} x_{i+(\nu-1)\frac{L}{2}}^{\nu} \, y_{i+(\nu-1)\frac{L}{2}+\tau}^{\nu}$, by applying periodic boundary conditions (Fig. 3(c)). For each time window ν we define the time delay τ_0^{ν} to correspond to the maximum in the absolute value of the cross-correlation function $C_{xy}^{\nu}(\tau)$ in this time window $\tau_0^{\nu} = \tau|_{|C_{xy}^{\nu}(\tau)| \geq |C_{xy}^{\nu}(\tau')|} \; \forall \tau'$. Time periods of stable interrelation between two signals are represented by segments of approximately constant τ_0 in the newly defined series of time delays, $\{\tau_0^{\nu}\}_{\nu=1,\ldots,N_L}$ — e.g., the flat region in Fig. 3(d) corresponding to a period of stable coupling between heart rate and respiratory rate during light sleep. In contrast, absence of stable coupling between the signals is characterized by large fluctuations in τ_0, as shown in the gray-shaded region in Fig. 3(d) corresponding to deep sleep.
(3.) We identify two systems as linked if their corresponding signals exhibit a time delay that does not change by more than ± 1 sec for several consecutive time windows ν. We track the values of τ_0 along the series $\{\tau_0^{\nu}\}$: when for at least four out of five consecutive time windows ν (corresponding to a period of 5×30 sec) the time delay remains in the interval $[\tau_0 - 1, \tau_0 + 1]$ these segments are labeled as stable. This procedure is repeated for a sliding time window with
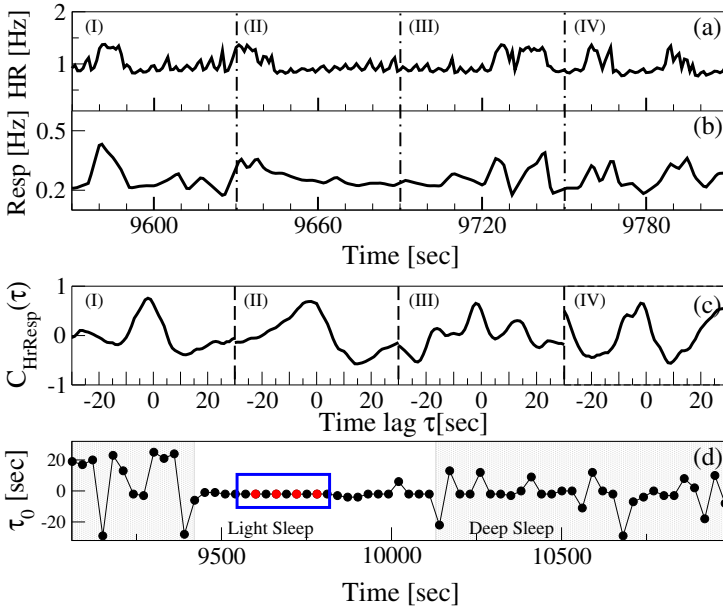
Fig. 3. Cardio-respiratory coupling: Time delay stability (TDS). Segments of (a) heart rate (HR) and (b) respiratory rate (Resp) normalized to zero mean and unit standard deviation in 60 sec time windows (I), (II), (III) and (IV), in order to remove trends in data and to obtain dimensionless signals. Synchronous bursts in the HR and Resp signal leading to pronounced cross-correlation within each time window as shown in (c), and stable time delay characterized by segments of constant τ_0 as shown in (d) — four red dots highlighted by a blue box in panel (d) represents the time delay for the 4 time windows. Note the transition from strongly fluctuating behavior in τ_0 to a stable time delay regime at the transition from deep sleep to light sleep at around 9400 sec (gray shaded area) in panel (d). The TDS analysis is performed on overlapping moving windows with a step of 30 sec represented by red and black dots in the blue box in panel (d). Long periods of constant τ_0 indicate strong physiological coupling.

a step size one along the entire series $\{\tau_0^\nu\}$. The % TDS is finally calculated as the fraction of stable points in the time series $\{\tau_0^\nu\}$.

Longer periods of TDS between the output signals of two systems reflect more stable interaction/coupling between these systems. Thus, the strength of coupling is determined by the percentage of time when TDS is observed: higher percentage of TDS corresponds to stronger coupling. To identify physiologically relevant interactions, we determine a significance threshold level for the TDS based on comparison with surrogate data derived from uncoupled systems, e.g., heart rate from subject A and respiratory rate from subject B. Only interactions characterized by TDS values above the significance threshold are considered.

The TDS method is general, and can be applied to diverse systems to identify and quantify links in networks of physiologic interactions that are not a priori known (Fig. 7). It is more reliable in identifying physiologic coupling compared

to traditional cross-correlation and cross-coherence analyses which are not suitable for heterogeneous and nonstationary signals, and are affected by the degree of auto-correlations embedded in these signals [28]. TDS is also suitable to identify coupling between systems that are not characterized by oscillatory output dynamics, where the phase-synchronization approach can not be applied.

In order to study interrelations and coupling between the brain and the cardiac and respiratory system, we extract the following time series from their output signals: the spectral power of seven frequency bands of the EEG in moving windows of 2 sec with a 1 sec overlap: δ waves (0.5-3.5 Hz), θ waves (4-7.5 Hz), α waves (8-11.5 Hz), σ waves (12-15.5 Hz), β waves (16-19.5 Hz) and $\gamma 1$ (20-33.5 Hz) and $\gamma 2$ (34-100 Hz) waves; heartbeat RR intervals and interbreath intervals are both re-sampled to 1 Hz (1 sec bins) after which values are inverted to obtain heart rate and respiratory rate. Thus, all time series have the same time resolution of 1 sec before the TDS analysis is applied. EEG data were recorded from 6 scalp locations: frontal left (Fp1), frontal right (Fp2), central left (C3), central right (C4), occipital left (O1) and occipital right (O2).

Applying the TDS method to these data we investigate the network of interactions between the brain, cardiac and respiratory system, and how this network changes with transition from one physiologic state to another (Figs. 7 and 8).

3   Results

3.1   Coexisting Forms of Coupling and Phase Transitions across Physiological States

To probe for coexistence of different forms of cardio-respiratory coupling we apply three different methods: (i) analysis of respiratory sinus arrhythmia (RSA), (ii) phase-synchronization analysis, and (iii) time delay stability analysis (TDS). These three methods quantify independent characteristics of the interaction between the cardiac and respiratory systems at different time scales: (i) amplitude of heart rate modulation during a breathing cycle (Fig. 1), (ii) phase-synchronized activity between the heart rate and the respiratory rate so that within a breathing cycle heartbeats occur at specific respiratory phases and this behavior is consistent for several consecutive breathing cycles (Fig. 2), and (iii) stable time delay in bursting activity of the heart and respiratory rate over long periods of time from several minutes to hours (Fig. 3).

Empirical studies have reported a strong variation in linear and nonlinear characteristics in both cardiac and respiratory dynamics with the sleep-wake cycle [16], across circadian phases [19, 29] and sleep-stage transitions [10–12, 30, 31], indicating significant changes in the regulatory mechanisms with transitions across physiologic states. Thus, we test whether cardio-respiratory coupling may also undergo phase transitions with transitions across physiologic states. Since sleep stages are well-defined physiologic states and are associated with distinct mechanisms of autonomic control [11, 12], we also investigate the strength of different forms of cardio-respiratory coupling during different sleep stages.
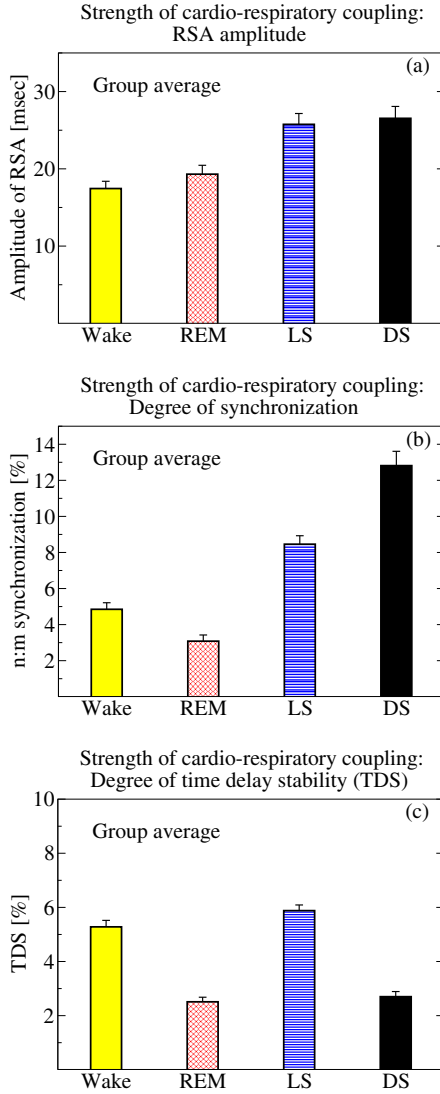
Fig. 4. Phase transitions in physiologic coupling across physiological states.
Stratification patterns in different measures of cardio-respiratory coupling with transitions across sleep stages indicate complex re-organization in physiological interaction during different physiologic states. Three independent forms of coupling — (a) Respiratory sinus arrhythmia (RSA), (b) Phase synchronization, and (c) Time delay stability (TDS) — show significantly different coupling strength during different sleep stages. Columns in each panel represent the average over a group of 189 healthy subjects; error bars correspond to the standard error. Phase synchronization and TDS coupling strength in (b) and (c) is estimated as the percent of data segments in the entire recording for a given sleep stage where heart rate and respiratory rate are phase-synchronized or exhibit TDS.

We find that the amplitude of RSA exhibits a pronounced and statistically significant stratification pattern across different sleep stages. The amplitude of RSA is lowest during wake periods and gradually increases during REM, light sleep and deep sleep. In particular, periods of non-REM sleep (light sleep and deep sleep) are characterized by $\approx 40\%$ higher RSA amplitude compared to REM and wake (Fig. 4(a)), indicating a strong dependence of this form of coupling on the underlying neuroautonomic control. With transition from wake to REM, light and deep sleep, the sympathetic tone of autonomic control decreases while the level of parasympathetic activity remains unchanged [11]. This yields a relative dominance of parasympathetic tone in cardiac and respiratory regulation, which in turn leads to lower respiratory rates in non-REM sleep associated with higher RSA amplitude. Indeed, experimental studies in healthy subjects show a decrease in the RSA amplitude with increasing respiratory frequency under paced respiration [20, 25]. However, we note that while the respiratory frequency decreases just with $\approx 6\text{-}8\%$ during transitions from wake to light and deep sleep, we find a highly nonlinear response in the RSA amplitude which increases with $\approx 40\%$ during these transitions.

Our analyses show that in addition to RSA cardio-respiratory interaction is characterized by two other forms of coupling — phase synchronization and time delay stability — which also exhibit a pronounced stratification in the strength of coupling across different sleep stages (Fig. 4(b,c)). However, in contrast to RSA cardio-respiratory phase synchronization is weaker during REM as compared to wake, while during light and deep sleep there is a dramatic increase in the degree of synchronization of $\approx 400\%$ compared to REM (Fig. 4(b)). Notably, this form of cardio-respiratory coupling exhibits a factor of 10 stronger response to sleep-stage transitions compared to RSA.

While the sleep-stage stratification patterns for both forms of coupling, RSA and synchronization, show a relative separation between non-REM and REM sleep, we find a very different stratification pattern for the strength of TDS: (i) much higher degree of TDS during wake and light sleep compared to REM and deep sleep, and (ii) comparable strength of TDS during wake and light sleep and during REM and deep sleep (Fig. 4(c)). Our empirical observation of significant difference in the degree of cardio-respiratory TDS coupling during light sleep compared to deep sleep is surprising, given the similarity in spectral, scale-invariant and nonlinear properties of cardiac and respiratory dynamics during light sleep and deep sleep [12, 30, 32] (light and deep sleep are traditionally classified as non-REM), and indicate that previously unrecognized aspects of cardiac and respiratory neuroautonomic regulation during sleep are captured by the TDS analysis.

Our investigations demonstrate the existence of three distinct forms of cardio-respiratory interaction that represent the dynamics at different time scales. Our findings of different stratification patterns indicate that these forms of coupling are independent and represent different aspects of physiologic interaction that are affected in a different way by changes in neuroautonomic control across physiologic states. Moreover, we find that these three forms of cardio-respiratory coupling are
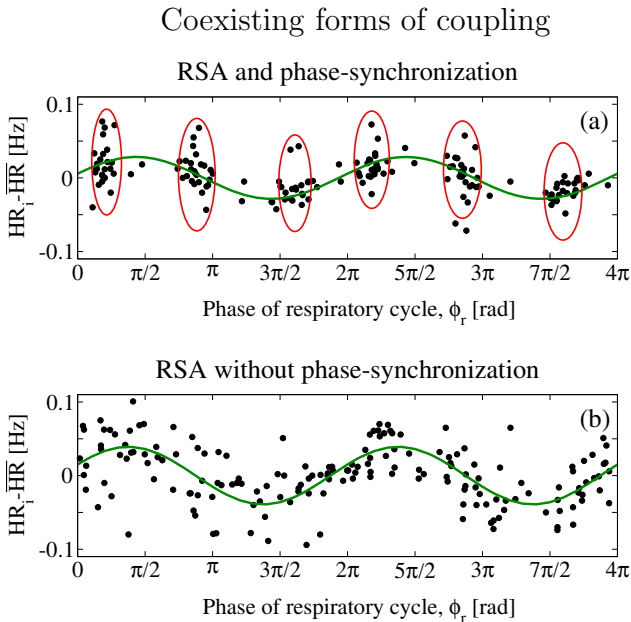
Coexisting forms of coupling

RSA and phase-synchronization

RSA without phase-synchronization

Fig. 5. Coexisting forms of cardio-respiratory coupling. Phase synchronization (CRPS) and respiratory sinus arrhythmia (RSA) represent different and independent forms of cardio-respiratory coupling. (a) While RSA leads to periodic modulation of the heart rate within each breathing cycle (green sinusoidal line) and is quantified by the amplitude of the heart rate modulation, CRPS leads to clustering of heartbeats at certain phases ϕ_r of the breathing cycle (red ovals). Shown are consecutive heartbeats over a period of 200 sec. The x-axis indicates the phases ϕ_r of the breathing cycle where heartbeats occur, and the y-axis indicates the deviation of the heart rate (inversed heartbeat intervals) from the mean heart rate $\overline{HR}$ within a given breathing cycle. Instantaneous heart rates are plotted over pairs of consecutive breathing cycles, $\phi_r \in [0, 4\pi]$, to better visualize rhythmicity. Data are selected from a subject during deep sleep. (b) For the same subject as in (a), instantaneous heart rates from another period of 200 sec also during a deep sleep episode are plotted over pairs of consecutive breathing cycles. Data show well-pronounced RSA with a similar amplitude as in (a), however, heartbeats are homogeneously distributed across all phases of the respiratory cycles, indicating absence of CRPS.

not continuously present and are not of constant strength but are rather transient and intermittent with "on" and "off" periods. Indeed, cardio-respiratory phase synchronization is usually observed in relatively short epochs rarely exceeding 100 sec in duration (Fig. 6). Even for the same subject within the same sleep stage, we find time periods when synchronization is not present (Fig. 5), indicating that "on" and "off" switching of this form of cardio-respiratory interaction is not always triggered by transitions across physiological states. Further, the total time when cardio-respiratory phase synchronization is observed even under controlled conditions in resting subjects is a relatively small fraction of the entire duration of the

recordings [33]. Moreover, some subjects may even not exhibit cardio-respiratory phase synchronization [33]. Our cardio-respiratory phase synchronization analysis shows that most of the synchronization epochs are of 20–45 sec duration (Fig. 6). Further, we find that for each subject the total sum of the synchronization epochs does not exceed 20–25% of the entire sleep duration or of the duration of the individual sleep stages, indicating that the cardio-respiratory coupling, as manifested by phase synchronization, is not stable in time.
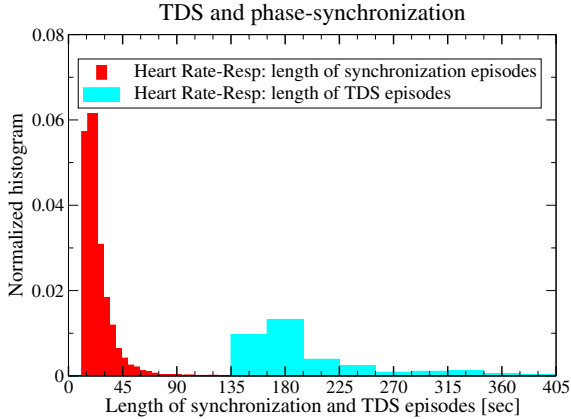
Coexisting forms of coupling

Fig. 6. Coexisting forms of cardio-respiratory coupling. Phase synchronization (CRPS) and time delay stability (TDS) probe the coupling at different time scales. Probability distributions of the length of cardio-respiratory phase synchronization epochs (red color) and of cardio-respiratory TDS epochs (light-blue color) indicating significant difference in the average epoch length. Thus, different aspects of cardio-respiratory coupling are captured by these two measures. However, both measures reflect transient changes in cardio-respiratory coupling with "on" and "off" periods even within a single sleep stage, where the "on" periods form only a fraction of the entire heart rate and respiratory recordings. Results are obtained from 189 healthy subjects, taking into account all sleep stages during a one-night sleep period.

The amplitude of RSA, another measure of cardio-respiratory coupling also continuously changes with breathing frequency and sympatho-vagal balance [20, 25], and under certain conditions RSA is even absent. Thus, the strength of RSA as a representative measure of cardio-respiratory coupling is also not stable in time. Finally, we find such intermittent behavior also in the TDS measure which probes cardio-respiratory coupling at larger time scales above 2 min. We note that TDS is a more stringent condition to quantify cardio-respiratory coupling, since TDS epochs longer than 2 min are more rare than the epochs of $\approx$ 20–45 sec typical for phase synchronization (Fig. 6). Indeed, our analyses show that most of the TDS epochs for the cardio-respiratory interaction are of 150–220

sec duration (Fig. 6). Since, epochs of TDS shorter than 2 min are neglected, we have a lower cardio-respiratory TDS (not exceeding $\approx$ 7% for the entire recording) compared to what we find for phase synchronization (Fig. 4(b,c)). We note that our choice of a 2 min window over which TDS is determined is not arbitrary because this is the minimal size window over which results obtained from the TDS method applied to real data are significantly different (t-test: $p < 10^{-3}$) from the results obtained based on surrogate data, where signals from one subject are paired with signals from different subjects.

The presence of "on" and "off" periods in the interaction between heart rate and respiration, where relatively short episodes of effective interrelation are separated by periods of no interrelation, is observed in all three independent measures — degree of phase synchronization, RSA and TDS — and indicates an intermittent nature of the coupling between these two systems. Importantly however, these intermittent dynamics do not always indicate that when one form of coupling is "on" the others must be "off". Rather our analysis shows that two or more forms of cardio-respiratory coupling can simultaneously coexist during the same time period within a given physiologic state (Figs. 5 and 6).

3.2   Networks of Physiologic Interaction

To study how different organ systems interact as a network, we apply the TDS method [23] to probe interactions between the brain, cardiac and respiratory systems, and how these interactions change across physiological states. Because brain dynamics are characterized by EEG signals with different spectral frequencies dominant at different scalp locations and during different physiological states, the TDS method allows us to study how bursts in EEG frequency bands from certain brain areas are coupled with corresponding bursts in the heart and respiratory rate.

We consider six scalp locations represented by EEG channels: frontal left (Fp1), frontal right (Fp2), central left (C3), central right (C4), occipital left (O1) and occipital right (O2). For each EEG channel, we estimate the coupling with the respiratory and cardiac systems by the degree of TDS for the following physiologically relevant EEG frequency bands: δ (0.5-3.5 Hz), θ (4-7.5 Hz), α (8-11.5 Hz), σ (12-15.5 Hz), β (16-19.5 Hz), $\gamma 1$ (20-33.5 Hz) and $\gamma 2$ (34-100 Hz). We represent each brain-respiration and brain-heart link in the network by the average of the TDS values obtained from all 7 frequency bands.

We find that the network of brain, respiratory and cardiac interactions exhibits different topology during different sleep stages. Specifically, we find that the physiologic network is characterized by high connectivity during wake and light sleep, lower connectivity during REM and is "disconnected" (below threshold TDS link strength) during deep sleep (Fig. 7). Such transitions in network structure indicate strong relation between network topology and physiologic function. Traditionally, differences between sleep stages are attributed to modulation in the sympatho-vagal balance with dominant sympathetic tone during wake and REM [32]: spectral, scale-invariant and nonlinear characteristics of the dynamics of individual physiologic systems indicate higher degree of temporal correlations
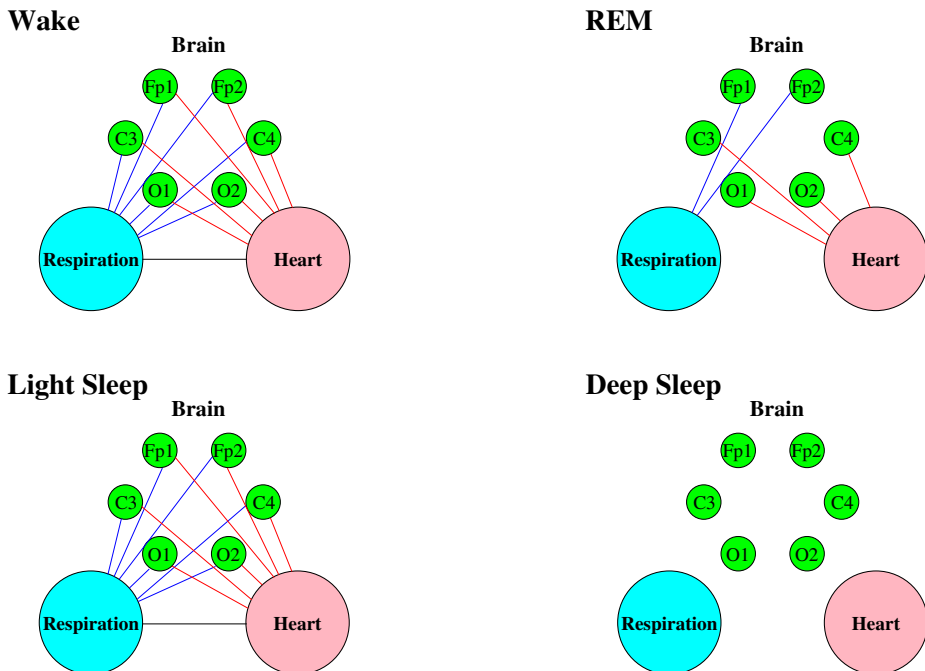
Network of physiologic interactions

Fig. 7. Phase transitions in network of interactions between physiological organ systems. Networks of cardiac, respiratory and brain interactions during different sleep stages. Different brain areas are represented by frontal (Fp1 and Fp2), central (C3 and C4) and occipital (O1 and O2) EEG channels. The strength of the links between pairs of systems is determined based on the TDS measure shown in Fig. 3. Plotted are only links the strength of which exceeds 50% of the maximum TDS value for all sleep stages: 7.5% TDS threshold for brain-heart links, 2% for brain-respiration links, and 3% for heart-respiration links. There is a pronounced network re-organization with transition from one sleep stage to another. Remarkably network connectivity is very different for light sleep and deep sleep although both sleep stages correspond to non-REM sleep. A similar contrast is observed between wake and REM. Networks are obtained from 8-hour recordings during sleep by averaging over a group of 36 healthy subjects.

and nonlinearity during wake and REM compared to non-REM (light and deep sleep) where physiologic dynamics exhibit weaker correlations and loss of non-linearity [12, 17, 30]. In contrast, the network of physiologic interactions shows a completely different picture: the network characteristics during light sleep are much closer to those during wake and very different from deep sleep (Fig. 7). Further, we find that not only network connectivity but also the overall strength of physiologic interactions is significantly higher during wake and light sleep, intermediate during REM and much lower during deep sleep (Fig. 8). Thus,
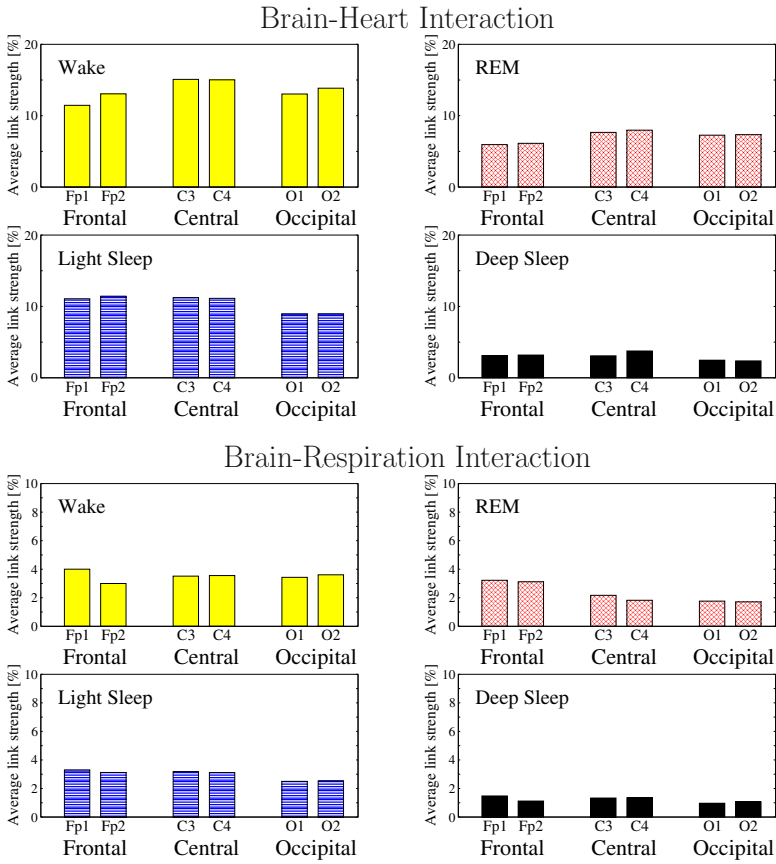
Fig. 8. Sleep-stage stratification pattern in the strength of network links between organ systems. Histograms show group averaged TDS links strength during different sleep stages for brain-heart (top four panels) and brain-respiration interaction (bottom four panels). Cardio-respiratory links strength for different sleep stages is shown in Fig. 4(c). A consistent stratification pattern with higher links strength during wake and light sleep compared to REM and deep sleep is observed for all pairs of coupling between brain, heart and respiration. Note that for all sleep stages, the brain-heart coupling strength as measured by TDS is consistently more than twice higher compared to the brain-respiration coupling. Histograms are obtained from 8-hour recordings during sleep by averaging over the same group of 36 healthy subjects as in Fig. 7.

our empirical observations indicate that while sleep-stage related modulation in sympatho-vagal balance plays a key role in regulating individual physiologic systems, it does not account for the physiologic network topology and dynamics across sleep stages, showing that the proposed TDS network approach captures principally new information.

We note that TDS quantifies the stability of coupling over large time scales. Absence of a link in the physiologic networks shown in Fig. 7 does not mean absence of coupling but rather that this coupling is present only for a small fraction of the data recordings. Specifically, networks links are not show when TDS is below the threshold value of 7.5% for brain-heart links, 2% for brain-respiration links, and 3% for heart-respiration links. Further, our investigations of the links strength in the physiologic networks show that brain-heart links as measured by the TDS are more than twice stronger than the brain-respiration links (Fig. 8), while the heart-respiration link is of intermediate strength (Fig. 4(c)). Notably this order in network links strength between the brain, heart and respiratory systems is preserved for all sleep stages. Remarkably, the sleep-stage stratification pattern we find for network connectivity, with high number of links during wake and light sleep, lower connectivity during REM and lowest during deep sleep (Fig. 7), is also present in the links strength — we find strongest links during wake and light sleep, weaker during REM and weakest links during deep sleep (Figs. 8 and 4(c)). Finally, our network analysis demonstrates a certain degree of heterogeneity in the network links strength between different brain areas and the heart and respiratory systems: frontal EEG channels show stronger coupling with respiration while central and occipital channels exhibit stronger coupling with the cardiac system. This heterogeneity in links strength is tentatively present at all sleep stages but most pronounced during REM (Fig. 8).

4   Conclusion

Utilizing concepts and methods from nonlinear dynamics, we demonstrate that the communication between pairs of physiologic organ systems can be facilitated by different forms of coupling. Considering the cardiac and respiratory systems, we show that there are three forms of coupling — respiratory sinus arrhythmia, phase synchronization and time delay stability — which are independent from each other and act on different time scales. Further, the strength of these forms of cardio-respiratory coupling changes with transitions across physiologic states such as sleep stages and exhibit markedly different sleep-stage stratification patterns. We find that all these forms of physiologic interaction are of transient nature with intermittent "on" and "off" periods, and can simultaneously coexist while at the same time representing different aspects of physiologic coupling and neuroautonomic regulation of the cardiac and respiratory systems. We extend these investigations to a network of physiologic interactions between the brain, cardiac and respiratory systems, and we uncover a strong relationship between network connectivity, patterns in network links strength and physiologic function. Studying the evolution of the physiologic network across distinct physiologic states such as wake, light sleep, deep sleep and REM, we show that physiologic networks exhibit pronounced phase transitions associated with reorganization in network structure and links strength in response to changes in the underlying neuroautonomic regulation. Our investigations are first steps towards understanding the network of communications between organ systems and developing a new field, Network Physiology.

References

1. Ivanov, P.C., Rosenblum, M.G., Peng, C.K., Mietus, J., Havlin, S., Stanley, H.E., Goldberger, A.L.: Scaling behaviour of heartbeat intervals obtained by wavelet-based time-series analysis. Nature 383, 323–327 (1996)
2. Ivanov, P.C., Amaral, L.A.N., Goldberger, A.L., Havlin, S., Rosenblum, M.G., Stanley, H.E., Struzik, Z.: From 1/f Noise to Multifractal Cascades in Heartbeat Dynamics. Chaos 11, 641–652 (2001)
3. Ivanov, P.C., Chen, Z., Hu, K., Stanley, H.E.: Multiscale aspects of cardiac control. Physica A 344, 685–704 (2004)
4. Bartsch, R., Hennig, T., Heinen, A., Heinrichs, S., Maass, P.: Statistical analysis of fluctuations in the ECG morphology. Physica A 354, 415–431 (2005)
5. Bartsch, R., Plotnik, M., Kantelhardt, J.W., Havlin, S., Giladi, N., Hausdorff, J.M.: Fluctuation and synchronization of gait intervals and gait force profiles distinguish stages of Parkinsons disease. Physica A 383, 455–465 (2007)
6. Ivanov, P.C., Ma, Q.D.Y., Bartsch, R.P., Hausdorff, J.M., Amaral, L.A.N., Schulte-Frohlinde, V., Stanley, H.E., Yonseyama, M.: Levels of complexity in scaleinvariant neural signals. Phys. Rev. E 79, 041920 (2009)
7. Ivanov, P.C., Amaral, L.A.N., Goldberger, A.L., Stanley, H.E.: Stochastic feedback and the regulation of biological rhythms. Europhys. Lett. 43, 363–368 (1998)
8. Ashkenazy, Y., Hausdorff, J., Ivanov, P.C., Stanley, H.E.: A stochastic model of human gait dynamics. Physica A 316, 662–670 (2002)
9. Lo, C.C., Amaral, L.A.N., Havlin, S., Ivanov, P.C., Penzel, T., Peter, J.H., Stanley, H.E.: Dynamics of sleep-wake transitions during sleep. Europhys. Lett. 57, 625–631 (2002)
10. Ivanov, P.C.: Scale-invariant aspects of cardiac dynamics - Observing sleep stages and circadian phases. IEEE Eng. Med. Biol. 26, 33–37 (2007)
11. Schmitt, D.T., Stein, P.K., Ivanov, P.C.: Stratification pattern of static and scaleinvariant dynamic measures of heartbeat fluctuations across sleep stages in young and elderly. IEEE Trans. Biomed. Eng. 56, 1564–1573 (2009)
12. Schumann, A.Y., Bartsch, R.P., Penzel, T., Ivanov, P.C., Kantelhardt, J.W.: Aging effects on cardiac and respiratory dynamics in healthy subjects across sleep stages. Sleep 33, 943–955 (2010)
13. Tass, P., Rosenblum, M., Weule, J., Kurths, J., Pikovsky, A., Volkmann, J., Schnitzler, A., Freund, H.: Detection of n: m phase locking from noisy data: Application to magnetoencephalography. Phys. Rev. Lett. 81, 3291–3294 (1998)
14. Pikovsky, A.S., Rosenblum, M.G., Kurths, J.: Synchronization: A Universal Concept in Nonlinear Sciences. Cambridge University Press, Cambridge (2001)
15. Schindler, K.A., Bialonski, S., Horstmann, M.T., Elger, C.E., Lehnertz, K.: Evolving functional network properties and synchronizability during human epileptic seizures. Chaos 18, 033119 (2008)
16. Ivanov, P.C., Bunde, A., Amaral, L.A.N., Havlin, S., Fritsch-Yelle, J., Baevsky, R.M., Stanley, H.E., Goldberger, A.L.: Sleep-wake differences in scaling behavior of the human heartbeat: analysis of terrestrial and long-term space flight data. Europhys. Lett. 48, 594–600 (1999)

17. Kantelhardt, J.W., Ashkenazy, Y., Ivanov, P.C., Bunde, A., Havlin, S., Penzel, T., Peter, J.H., Stanley, H.E.: Characterization of sleep stages by correlations in the magnitude and sign of heartbeat increments. Phys. Rev. E 65, 051908 (2002)
18. Karasik, R., Sapir, N., Ashkenazy, Y., Ivanov, P.C., Dvir, I., Lavie, P., Havlin, S.: Correlation differences in heartbeat fluctuations during rest and exercise. Phys. Rev. E 66, 062902 (2002)
19. Ivanov, P.C., Hu, K., Hilton, M.F., Shea, S.A., Stanley, H.E.: Endogenous circadian rhythm in human motor activity uncoupled from circadian influences on cardiac dynamics. Proc. Natl. Acad. Sci. USA 104, 20702–20707 (2007)
20. Angelone, A., Coulter, N.A.: Respiratory sinus arrhythmia: A frequency dependent phenomenon. J. Appl. Physiol. 19, 479–482 (1964)
21. Bartsch, R.P., Schumann, A.Y., Kantelhardt, J.W., Penzel, T., Ivanov, P.C.: Phase transitions in physiologic coupling. Proc. Natl. Acad. Sci. USA 109, 10181–10186 (2012)
22. Sornette, D.: Critical phenomena in natural sciences. Chaos, fractals, selforganization, and disorder — Concepts and tools, 2nd edn. Springer, Berlin (2004)
23. Bashan, A., Bartsch, R.P., Kantelhardt, J.W., Havlin, S., Ivanov, P.C.: Network physiology reveals relations between network topology and physiological function. Nat. Commun. 3, 702 (2012)
24. Dorogovtsev, S.N., Mendes, J.F.F.: Evolution of networks. Advances in Physics 51, 1079–1187 (2002)
25. Song, H.S., Lehrer, P.M.: The effects of specific respiratory rates on heart rate and heart rate variability. Appl. Psychophysiol. Biofeedback 28, 13–23 (2003)
26. Rosenblum, M.G., Pikovsky, A.S., Kurths, J.: Phase synchronization of chaotic oscillators. Phys. Rev. Lett. 76, 1804–1807 (1996)
27. Xu, L., Chen, Z., Hu, K., Stanley, H.E., Ivanov, P.C.: Spurious detection of phase synchronization in coupled nonlinear oscillators. Phys. Rev. E 73, 065201 (2006)
28. Podobnik, B., Fu, D.F., Stanley, H.E., Ivanov, P.C.: Power-law autocorrelated stochastic processes with long-range cross-correlations. Eur. Phys. J. B 56, 47–52 (2007)
29. Hu, K., Ivanov, P.C., Hilton, M.F., Chen, Z., Ayers, R.T., Stanley, H.E., Shea, S.A.: Endogenous circadian rhythm in an index of cardiac vulnerability independent of changes in behavior. Proc. Natl. Acad. Sci. USA 101, 18223–18227 (2004)
30. Bunde, A., Havlin, S., Kantelhardt, J.W., Penzel, T., Peter, J.H., Voigt, K.: Correlated and Uncorrelated Regions in Heart-Rate Fluctuations during Sleep. Phys. Rev. Lett. 85, 3736–3739 (2000)
31. Kantelhardt, J.W., Penzel, T., Rostig, S., Becker, H.F., Havlin, S., Bunde, A.: Breathing during REM and non-REM sleep: correlated versus uncorrelated behaviour. Physica A 319, 447–457 (2003)
32. Otzenberger, H., Gronfier, C., Simon, C., Charloux, A., Ehrhart, J., Piquard, F., Brandenberger, G.: Dynamic heart rate variability: A tool for exploring sympathovagal balance continuously during sleep in men. Am. J. Physiol. 275, H946–H950 (1998)
33. Schäfer, C., Rosenblum, M.G., Kurths, J., Abel, H.H.: Heartbeat synchronized with ventilation. Nature 392, 239–240 (1998)